19th Australasian Fluid Mechanics Conference
Melbourne, Australia
8-11 December 2014

Validation of a Three-dimensional CFD Analysis of Foil Bearings with Supercritical CO_2

K. Qin, I.H. Jahn and P.A. Jacobs

Queensland Geothermal Energy Centre of Excellence
School of Mechanical and Mining Engineering
The University of Queensland, St Lucia 4072, QLD, Australia

Abstract

Foil bearings are an integral part of oil-free turbomachines which have been selected as a potential technology to enable cost efficient Supercritical Carbon Dioxide Brayton cycle for solar power application. Using high pressure CO_2 as the operating fluid means that within the film Reynolds numbers in the highly turbulent regime are observed, therefore, using traditional simulation tools, such as two-dimensional Reynolds equation, derived for simulating bearing operating with laminar flow is not appropriate. The resulting turbulence enhances hydrodynamic load capacity and increases frictional losses. In this study, some improvements such as moving wall and periodic boundary conditions to the UQ in-house CFD code Eilmer are presented. These are verified using Taylor-Couette flow, and axisymmetric and wavy Taylor vortices are simulated under different Taylor number. A hydrostatic air thrust bearing with steady-state behaviour is also studied, which shows good agreement with the results from modified Reynolds equation. Finally, a preliminary Three-Dimensional Computational Fluid Dynamic simulation of a foil bearings is presented. A rigid foil bearing is studied with ambient air and high pressure CO_2 as operating fluid, respectively and the lift force and power loss are compared with the results from Reynolds equation.

Introduction

The supercritical CO_2 (sCO_2) closed Brayton cycle, which uses high pressure CO_2 as its working fluid, is an alternative to conventional steam turbines, offering the potential for better overall economics due to a higher electrical conversion efficiency and lower capital cost. Dostal et al. [1] showed that the sCO_2 cycle has a higher efficiency than the superheated steam cycle at temperatures above 470°C, which makes it suitable for nuclear power applications. sCO_2 cycle for solar thermal application has also been proposed [2, 3].

Before realizing sCO_2 cycles, a number of challenges need to be overcome, making this an active area of research. The key components of this cycles (turbine, compressor, stators, bearings, seal) need to be re-studied due to the new working fluid and especially the non-linear behaviour exhibited by sCO_2 [4, 5, 6]. Kuz et al. [4] studied one-dimensional design methodology for supercritical CO_2 compressor and turbine. Pecnik et al. [5] presented a three-dimensional CFD study of the impeller of a centrifugal compressor operating with sCO_2 in the thermodynamic region slightly above the vapor-liquid critical point. Kim et al. [6] provided CFD investigation of a centrifugal compressor with supercritical CO_2 as working fluid, the steady-state numerical predictions using the $k-\omega$ SST model were found to return satisfactory results in the case of sCO_2 operating condition, but the gas conditions were quite far from the critical point.

However, besides these key components, sCO_2 bearings design cannot be neglected. Many of early tests of sCO_2 cycle at Sandia used ball bearings to allow for testing. However, the ball bearings were expected to have a limited lifetime that varies from 20 hours to 2000 hours depending on the thrust load that was assumed [7], and then the design also included the option to operate with gas foil bearings. Conboy [8] presented a preliminary study of foil bearing with high pressure CO_2 as operating fluid, the Reynolds equation considering turbulence effect was solved, but the analysis of gas foil bearings was largely based on data reported by NASA Glenn Research Centre by DellaCorte and Bruckner [9], these correlations were developed for gases at low pressure and not for high pressure CO_2. High pressure CO_2 is far denser than air, less viscous compared to oil, and highly non-ideal, these factors present unique challenges in predictive modelling as compared to more conventional lubricants and applications, including the potential for turbulence in lubrication films.

In order to better understand the fluid behaviour in bearing chamber, a three-dimensional Computational Fluid Dynamic analysis method should be developed and validated. This paper demonstrates the suitability of Eilmer [10] for bearings simulation by verifying and validating it against analytical or experimental results. Taylor-Couette flow is used to verify the Moving wall and periodic boundary conditions. Hydrostatic air thrust bearing is employed to study the suitability of Eilmer in simulating the centrifugal inertia effect. Wavy thrust bearins is then used to test the suitability of Eilmer in simulating the performance of bearings with a typical geometry.

Test Cases

Taylor-Couette Flow

This test case is used to verify the non-zero rotational speed version of the Moving-Wall boundary condition. It selects some examples of compressible Taylor-Couette flow from Ref. [11] for an annulus with inner radius 215.5 mm and gap width 3.1 mm. The axial extent of the annulus is 5 times the gap width. The outer cylindrical surface (the housing) of the annulus was fixed and the inner surface (the rotor) was moving with a rotational speed of 27600 rpm. Two different pressures are simulated to cover a range of cases, with and without Taylor vortices. Other parameters used for the simulations are shown in Ref. [11].

For the intermediate pressure case, shown in figure 1, there are similar results of temperature and tangential velocity between Eilmer and other codes [11]. The Taylor number in this case is only 12, no vortices will be generated in this range. The profile for the tangential velocity is nearly linear and the temperature profile is nearly parabolic with a maximum slightly closer to the hotter wall as seen in the agreement between numerical schemes is good.

For the high pressure case, the Taylor number has exceeded a critical value and vortices aligned with the surface velocity of the rotor, made the gap fully three dimensional. Schlichting [16] suggested that as the Taylor number in incompressible flow ranges between 41.3 and 400, laminar flow with Taylor vortices would be observed. In this range, the flow can be further char-

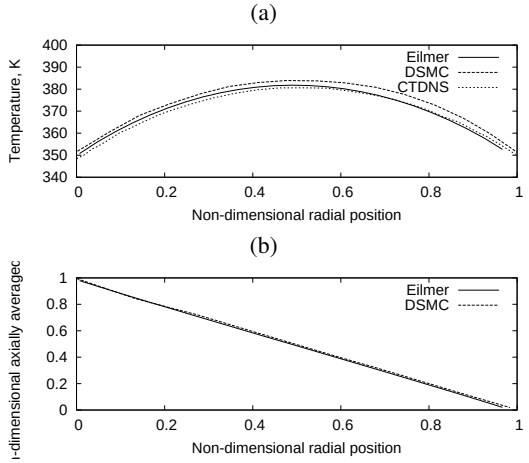

Figure 1: Comparison of temperature (a) and velocity (b) profiles in radial direction at intermediate pressure condition.

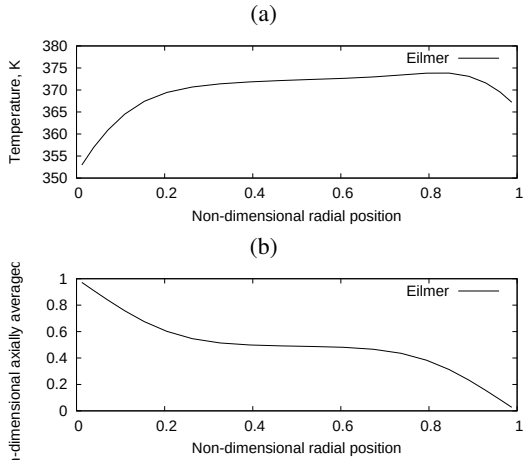

Figure 2: Temperature (a) and velocity (b) profiles in radial direction at Taylor-vortices case.

acterised as axisymmetric Taylor vortices, wavy Taylor vortices and others. However, the Taylor number for the transition from axisymmetric Taylor vortices to wavy vortices is not firmly established. For instance, the transition is theoretically predicted to occur at $\frac{T}{T_{crit}} = 1.1$ for aspect ratio $\eta = 0.85$ for infinitely long cylinders [12, 13], whereas experiments indicate a range of higher values between 1.14 and 1.31 for $\eta = 0.80 - 0.90$, depending on experimental conditions [14]. Although the CTDNS code is written for fully three-dimensional flow geometries, the flow is considered 2D axisymmetric, and then a stable axisymmetric vortices is simulated in Ref. [11].

If the rotational speed of the rotor is reduced to 18400 rpm, other parameters remain the same with high pressure case in Ref. [11], the axisymmetric vortices can be simulated. The velocity profile (averaged over the axial direction) has changed to an S-shapes curve in figure 2. This velocity profile characterise a flow with a higher gradient at the walls, due to enhanced radial transport of fluid induced by the vortices. The axially averaged temperature profile is much flatter than parabolic of the lower Taylor number cases. This averaged shape also exhibits steeper gradient at the walls, which induce a high heat flux. Again, these changes are due to the presence of vortices and the associated increase in radial transport of momentum and energy across the gap.

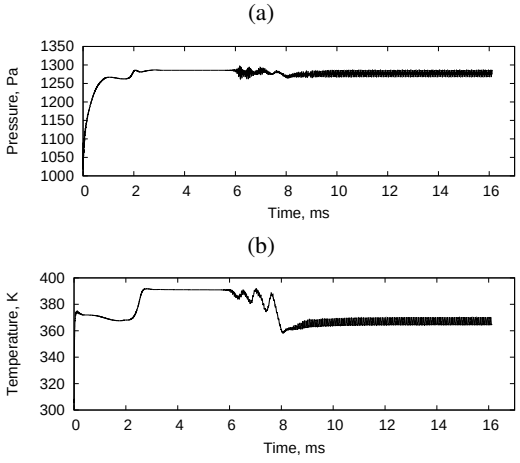

Figure 3: Parameters variation of Taylor-Couette Flow at high pressure condition; (a): pressure; (b): temperature.

Back to the rotational speed of 27600 rpm in Ref. [11], the ratio of Taylor number at high pressure case to critical Taylor number is 2.22, and the flow will eventually evolve into instable wavy vortices, figure 3 monitored temperature and pressure variation with simulation time in Eilmer, where the temperature and pressure will oscillate with a certain frequency, eventually.

Hydrostatic Air Thrust Bearing

With high density CO_2 as operating fluid, centrifugal inertial effect cannot be ignored, this hydrostatic air thrust bearing is used to verify the suitability of Eilmer in simulating thrust bearing as well as modelling centrifugal inertia force. Garratt et al. [15] considered the centrifugal inertia effects in high-speed hydrostatic air thrust bearings, a modified Reynolds equation for compressible flow is used to model the dynamics of pressurised air bearings in a simplified axisymmetric geometry. The basic air-flow characteristics were analysed for various bearing number λ under steady-state condition when the bearing faces are fixed at a constant distance, the modified Reynolds equation is defined in Ref. [15].

Pressure profiles for an inward pressurised bearing are shown in figure 4, corresponding to wide and narrow bearings, respectively. At low rotation speeds, the inward pressurisation gives a smoothly decreasing pressure from the outer to inner radii. For sufficiently high speeds, the pressure becomes sub-ambient towards the outer edge. But for the narrow bearing, the pressure remains above the ambient internal pressure for the same bearing number. As is shown in figure 4. The pressure distribution of CFD results from Eilmer shows good agreements with analytical results of Reynolds Equation. Eilmer has correctly captured the inertial effects, which are the cause of the dip in pressure observed with wide bearings. These results indicate that the narrow configuration is less sensitive to the effect of rotation than the wide bearing.

For an inward pressurised bearing, the positive pressure gradient generates a positive component of the stream function that, in the absence of high-speed rotation, will result in a purely inward flow. However, with rotational effects, the flow near the rotor is outwards, and this region of outward flow increases in size for higher rotation speeds, and zero radial velocity position line is used to mark the boundary between inward and outward flow. figure 5 shows the comparison result of zero radial velocity position between Eilmer and Reynolds equation, and comparison results are good, which means Eilmer can accurately

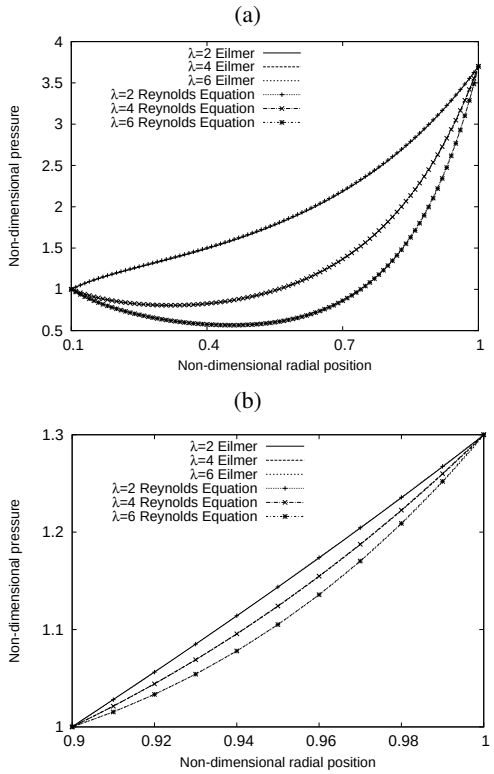

Figure 4: Steady pressure distribution in an inward bearing for different bearing number: (a): wide bearing; (b): narrow bearing.

capture the inward and outward flow.

Wavy Thrust Bearing

This test case is used to study the suitability of Eilmer in simulation of pressure distribution in bearings with complex pad geometry. The modeling of a wavy thrust bearing has been studied by Zhao et al. [17] with Reynolds equation. The numerical simulation of a self-acting thrust bearing has been developed using a system of two circular discs moving relative to each other. The geometry is shown in figure 6(a), the other parameters for this wavy thrust bearing is defined in table . High pressure CO_2 is used as working fluid for case 1, and the ambient condition is 1.4 MPa and 300 K as suggested by Sandia's test results [8]. The inner and outer surfaces are regarded as

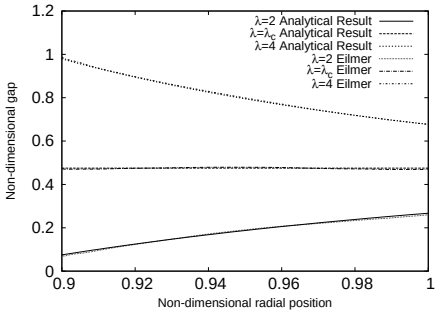

Figure 5: Comparison of zero radial velocity line at different bearing number.

Outer radius of discs	50.8 mm
Inner radius of discs	25.4 mm
Nominal average clearance, h_c	0.010 mm
Wave amplitude, g	6.35 μm
Rotational speed	25000 rpm
Pad angular extent	45 deg

Table 1: Wavy thrust bearing physical and operational characteristics.

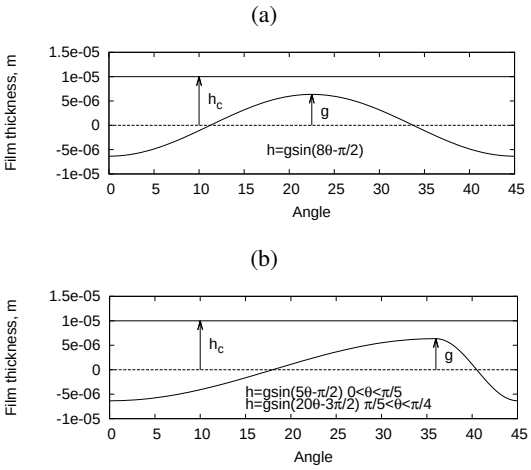

Figure 6: Schematic of film thickness for 45 degree wavy bearing pad; (a): symmetric wavy geometry; (b): 4:1 ratio wavy geometry.

modelled as moving and fixed temperature wall, respectively, other two surfaces are connected with periodic boundary condition. The grid independence study for Eilmer has been done as well as finite difference code for Reynolds equation. figure 7(a) shows comparison results of pressure distribution at mean radius between Eilmer and Reynolds equation, The good agreement between Reynolds equation and Eilmer demonstrates the ability of Eilmer to correctly simulate wavy bearings.

To study a more foil bearing like geometry, characterised by a long compression ramp, followed by an almost instantaneous expansion, case 2 explores the flow in wavy bearing with a skewed sin-wave geometry. The ratio of compression to expansion part is now changed into 4:1 shown in figure 6(b). The resulting pressure measured at the bearing mean radius for Reynolds equation and Eilmer are shown in figure 7(b). Agreement continues to be good.

The comparison results of lift force and friction torque integrated from Reynolds equation and Eilmer is shown in table . The relative error between Eilmer and Reynolds equation for these two cases is almost the same, 70 N for lift force and 14 Nmm for friction torque, this further verifies that Eilmer can be used to simulation bearing performance. However, in reality,

Case	Lift force Eilmer N	Lift force Reynolds N	Friction torque Eilmer Nmm	Friction torque Reynolds Nmm
1	374.20	308.51	64.41	50.45
2	723.60	650.46	64.35	50.49

Table 2: Comparison results of lift force integrated from Reynolds equation and Eilmer.

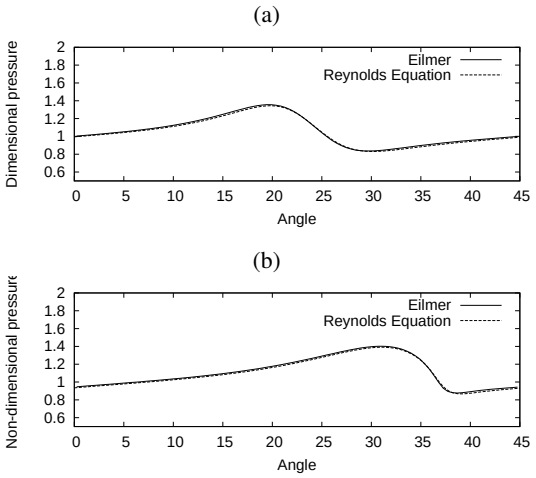

Figure 7: Comparison of pressure distribution at mean radius between Eilmer and Reynolds equation at high gap condition; (a): symmetric wavy geometry; (b): 4:1 ratio wavy geometry.

fixed temperature boundary condition can't be set to rotor as well as pad, and with high pressure CO_2 as working fluid, turbulence effect also can't be neglected, Reynolds equation might not be adequate when considering these effects, thus, CFD analysis should be addressed.

Conclusions

This paper demonstrates the development and validation of in-house CFD code Eilmer for foil bearing simulation, and three different test cases were simulated to verify the results from Eilmer. The moving wall and periodic boundary conditions are verified with Taylor Couette flow, while the suitability of Eilmer in simulating centrifugal inertia force is verified by high speed air thrust bearings. For wavy thrust bearings with more complex geometry, CFD results show good agreement compared to Reynolds equation for symmetric wavy as well as high compression geometry. However, the rotor and pad can't be simply modelled as fixed temperature wall, and turbulence effect also can't be neglected. Reynolds equation might not be adequate when considering these effects, thus, CFD analysis should be implemented to study fluid behaviour in bearing chamber.

Acknowledgements

This research was performed as part of the Australian Solar Thermal Research Initiative (ASTRI), a project supported by Australian Government. The author, Kan Qin, would also like to thank China Scholarship Council (CSC) for the financial support.

References

[1] Dostal, V., Driscoll, M.J. and Hejzlar, P., A Supercritical Carbon Dioxide Cycle for Next Generation Nuclear Reactors, *MIT Report* , No. MIT-ANP-TR-100, 2004.

[2] Turchi, C.S., Ma, Z., Neises, T.W. and Wanger, M.J., Thermodynamic Study of Advanced Supercritical Carbon Dioxide Power Cycles for COncentrating Solar Power System, *Journal of Solar Energy Engineering*, **135**, 2013, 041007.

[3] Gurgenci, H., Supercritical CO_2 Cycles Offer Experience Curve Opportunity to CST in Remote Area Markets, *Energy Procedia*, **49**, 2014, 1157–1164.

[4] Kuz, B. and Neksa P., Development of One-dimensional Model for Initial Design and Evaluation of Oil-free CO_2 Turbo-compressor, *International Journal of Refrigeration*, **36**, 2013, 2079–2090.

[5] Pecnik, R., Rinaldi, E. and Colonna, P., Computational Fluid Dynamics of a Radial Compressor Operating with Supercritical CO_2, *Journal of Engineering for Gas Turbines and Power*, **134**, 2012, 122301.

[6] Kim, S.G., Lee, J., Ahn, Y., Lee, J.I., Addad, Y. and Ko, B., CFD Investigation of a Centrifugal Compressor Derived from Pump Technology for Supercritical Carbon Dioxide as a Working Fluid, *The Journal of Supercritical Fluids*, **86**, 2014, 160–171.

[7] Wright, S.A., Radel, R.F., Vernon, M.E., Rochau, G.E. and Pickard, P.S., Operation and Analysis of a Supercritical CO_2 Brayton Cycle, *Sandia Report* , No. SAND2010-0171, 2010.

[8] Conboy, T.M., Real Gas Effects in Foil Thrust Bearings Operating in the Turbulent Regime, *Journal of Tribology*, **135**, 2013, 031703.

[9] DellaCorte, C. and Bruckner, R.J., Remaining Technical Challenges and Future Plans for Oil-Free Turbomachinery, *Journal of Engineering for Gas Turbines and Power*, **133**, 2011, 042502.

[10] Gollan, R.J. and Jacobs, P.A., About the Formulation, Verification and Validation of the Hypersonic Flow Solver Eilmer, *International Journal for Numerical Methods in Fluids*, **73**, 2013, 19–57.

[11] Larignon, B., Marr, K. and Goldstein, D.B., Monte Carlo and Naiver-Stokes Simulations of Compressible Taylor-Couette Flow, *AIAA Journal of Thermophysics and Heat Transfer*, **20**, 2006, 544–551.

[12] DiPrima, R.C., Eagles, P.M. and Ng, B.S., The Effect of Radius Ratio on the Stability of Couette Flow and Taylor Vortex Flow, *Phys. Fluids*, **27**, 1984, 2403–2411.

[13] Jones, C.A., The Transition to Wavy Taylor Vortices, *J. Fluid Mech.*, **157**, 1985, 135–162.

[14] Wereley, S.T. and Lueptow, R.M., Azimuthal Velocity in Supercritical Circular Couette Flow, *Exp. Fluids*, **18**, 1994, 1–9.

[15] Garratt, J.E., Hibberd, S. and Cliffe, K.A., Centrifugal Inertia Effects in High-speed Hydrostatic Air Thrust Bearings, *J. Eng. Math.*, **76**, 2012, 59–80.

[16] Schlichting, H., *Boundary Layer Theory*, McGraw–Hill, 1979.

[17] Zhao, H., Choy, F.K. and Braun, M.J., Modeling and Analysis of a Wavy Thrust Bearing, *Tribology Transactions*, **45**, 2002, 85–93.